SUBSYNCHRONOUS INSTABILITY OF A GEARED CENTRIFUGAL COMPRESSOR OF OVERHUNG DESIGN

J. H. Hudson and L. J. Wittman
Allis-Chalmers Corp.
Milwaukee, Wisconsin 53201

INTRODUCTION

This paper presents the original design analysis and shop test data which were obtained for this compressor. Also included are field test data, subsequent rotor dynamics analysis, modifications, and final rotor behavior.

BASIC COMPRESSOR CHARACTERISTICS

The subject unit is a three-stage (poster) air compressor, with impellers mounted on the extensions of a twin pinion gear, driven by an 8000-hp synchronous motor. The motor speed is 1200 rpm, with speeds of 8057 rpm on the low-speed pinion and 9400 rpm on the high-speed pinion. The compressor is rated at approximately 40 000 acfm and an approximate discharge pressure of 100 psia under normal summer conditions of temperature and humidity. Operation of the process plant is basically constant weight flow at constant pressure.

At the time of design the compressor represented the highest horsepower and largest volume for a three-poster design that had been built by Allis-Chalmers. Four-poster designs had been built for higher horsepower levels using the same frame size.

SUMMARY OF ORIGINAL ROTOR DESIGN METHODS

According to usual practice for a compressor of this type the aerodynamic requirements were defined initially, thus establishing minimum pinion center distances to allow for casing clearance. The gear vendor then designed the gearing to satisfy power and ratio requirements in accordance with Allis-Chalmers' specifications, which included data on pinion extension details. After the pinion was designed to satisfy gearing and bearing loading requirements a rotor response evaluation of the pinions was performed.

At the time this compressor was designed, rotor analysis was limited to undamped critical speed and synchronous unbalance response analysis, both assuming a circular orbit (isotropic bearing properties).

Details of speeds, horsepower, bearing types, and loading, as well as the lubricant, are given in table 1.

Figure 1 is a pseudo-undamped critical speed map for the low-speed pinion. Because of unequal bearing properties the usual intersect point on this curve is not appropriate. The stiffness for the bearings range from 5×10^5 to 4×10^6 lb/in. A similar pseudo-mode shape plot is also presented in figure 2

for a stiffness of $1x10^6$ lb/in. Figure 3 is a synchronous unbalance response plot assuming unequal but constant bearing loadings with unbalance distribution to excite the first mode. Assumption of constant bearing loading and direction is not correct, as can be seen from figure 4; however, the program at that time could not accommodate variations of this type.

Figure 5 is an undamped critical speed map of the high-speed pinion with part- and full-load bearing stiffnesses superimposed. Figures 6 and 7 are mode shapes of the rotor at $1x10^6$- and $1x10^7$-lb/in bearing stiffnesses. This range encompasses the actual bearing stiffness. Figure 8 is a synchronous unbalance response plot with combined unbalance to excite the first and second modes. Based on the rotor dynamics analysis the compressor design was deemed acceptable and proceeded through manufacture.

SHOP TESTING

The compressor was mechanically and aerodynamically tested. The first stage was tested at atmospheric discharge conditions; therefore the low-speed pinion was loaded to approximately 45% of design horsepower. The high-speed pinion was tested with atmospheric inlet conditions and was loaded to approximately 35% of its rated load.

The compressor was equipped with radial proximity probes in the vertical direction only. Vibration was monitored by using a digital vector filter and real-time analyzer. The vibration spectrum for the low-speed pinion contained synchronous and low-level two-per-revolution signals at 0.65 and 0.1 mil, respectively, for the impeller end probe and 0.3 and 0.1 mil, respectively, for the thrust bearing end probe. The vibration spectrum for the high-speed pinion showed a synchronous component of 0.2 mil at both pinion probes and was virtually free of all nonsynchronous components. The vibration signals were tape recorded for quality assurance documentation. The compressor met mechanical and aerodynamic requirements and was shipped.

FIELD PERFORMANCE

Shortly after startup the compressor exhibited overall vibration levels of 1.0 to 1.5 mils. It was observed that nearly 0.75 mil existed at slow roll. Test tape recordings revaled that about 0.3 mil existed as electrical and mechanical runout when the unit was tested at the factory. The additional electrical runout was attributed to magnetic fields induced by welding cables that slung over the casing during installation.

During the early commissioning of the compressor the customer reported sporadic vibration behavior of the low-speed rotor. At periods the overall vibration level was around 1.5 mils and occasionally levels of 3 mils and greater were reported. Figure 9 reveals operating points where moderate and high vibration conditions existed. A test was conducted with the compressor guide vane fixed at 0° prewhirl. Test points were taken at flows from beyond the rated point to close to the surge limit of the compressor. The high flow points showed very little subsynchronous vibration (<0.1 mil); however, as the flow was decreased the subsynchronous component continued to increase until the subsynchronous component was approximately 1.5 mils, or 3 times the synchronous

level of vibration. A point of interest is that two levels of subsynchronous frequency appeared. Refer to figures 10 to 13, which depict the changing subsynchronous spectrum. It was apparent that a bounded subsynchronous instability existed in the rotor.

ANALYSIS OF FIELD DATA

Between the time when the compressor design was originally analyzed and the time of the field tests in which subsynchronous vibration was found, considerable improvements were made to Allis-Chalmers rotor dynamic analysis capabilities (refs. 1 and 2). This finite-element method of analysis enabled us to calculate undamped critical speeds with unequal bearing forces. Input of bearing forces to reflect external loading, such as gear reactions, was an added capability. Synchronous unbalance response was upgraded to account for possible bearing asymmetry. Rotor stability calculations were improved and made more convenient and less expensive. A pad assembly program was developed which enabled the development of a full matrix to represent bearing stiffness and damping for the stability analysis with a minimum of effort. Refer to figures 16 and 17, which reflect mode shape and response plots for the subject rotor with these capabilities.

The low-speed pinion was modeled by using these programs to gain insight into its base log decrement at operating conditions and subsequently to evaluate proposed modifications. The rotor model included the added weight of shrunk-on parts without any additional stiffening effect of these parts. The effective stiffness of the center section of the rotor, where significant difference in shaft diameters exists, was based on data presented in reference 5. A horsepower level was chosen for analysis based on aerodynamic data for a test point represented by figure 13. Bearing and gear manufacturer's quality records were procured. They revealed that the actual bearing diametral clearance ranged from 0.0075 to 0.0093 inch with preload between 0.2 and 0.4, respectively.

The modeled original configuration was analyzed without any calculated destabilizing force at the impeller. No attempt was made to make allowances for labyrinth seal effects or nebulous factors such as internal friction. This analysis resulted in a relatively sizable value of log decrement (table 2 and fig. 14). The frequency and mode shape were in good agreement with probe data from field tests. Several other cases were analyzed and are summarized here.

Destabilizing Forces

It was assumed that the primary cause of instability in the rotor was associated with aerodynamic destabilizing forces. Several levels were analyzed until a log decrement of 0.0 was obtained (fig. 18). As a point of reference the destabilizing force was calculated according to references 4 and 8 per the equation

$$Kxy = -Kyx = \frac{T}{2rh}$$

where

K_{xy}, K_{yx} aerodynamic destabilizing force represented as cross-coupled bearing stiffness, lb/in

T torque input to stage, in-lb

r impeller mean radius, in.

h blade height, in.

The computed value of the 0° guide vane instability (fig. 13) test point is 742.5 lb/in. The destabilizing value calculated to create a log decrement of 0.0 is approximately 16 000 lb/in, or 21.5 times the calculated value.

As a basic of comparison it was decided to use 16 000 lb/in for the remainder of the analysis.

Rotation of Existing Bearings

It was decided to determine the effects of rotating the journal bearings based on data presented in reference 6. An analysis was made for loading directly into the pivot and directly centered between the pivots. It was determined that rotation would be of little benefit. Refer to table 2 for summary details.

Increased Bearing Width

The effect of increased bearing width (1.0 L/D) was analyzed to establish if improvements in the log decrement could be made. Several combinations of diametral clearances and preload were evaluated for loading into the pivot. It was found that a lower preload (normally 0.2) and bearing clearances toward the upper range of the clearance range defined in table 2 would produce the best improvement in log decrement. The relative increase in log decrement for a bearing preload of 0.2 and an average diametral clearance of 0.0085 inch is presented in figure 18. Details are tabulated in table 2.

A run using the above preload and clearance (0.2 and 0.0085 in., respectively) was performed for load between pivots. A decrease in log decrement was found (table 2).

Reduction of Impeller Overhang

An analysis was performed of the bearings as designed and installed and the pinion as designed except for removing 2 inches from the shaft between the impeller and the impeller end bearing. The effect on the log decrement was a considerable improvement, as detailed in table 2.

Increase in Shaft Section Modulus

An analysis was made of the compressor rotor as designed except for increasing the pinion bearing diameter to 4.5 inches. The bearing L/D was maintained at 0.75 with an average preload of 0.2 and a clearance of 0.0095 inch. Again a considerable improvement was found in the log decrement, nearly equal to that for reducing the overhang. Details are listed in table 2.

Oil Viscosity Effects

A higher viscosity was used in the compressor to favor gear lubrication. The effects of viscosity changes were analyzed for the case of a bearing L/D equal to 1 with load into the pivot. As can be seen from the data in table 2 further increase in oil viscosity would either raise or lower the log decrement for this rotor.

ACTUAL FIELD MODIFICATIONS AND FIELD RETESTING

As a result of this analysis it was apparent that the most expedient modification to improve rotor stability is a bearing modification. A wider bearing (L/D = 1.0) with a nominal preload of 0.2 and clearance range of 0.0075 to 0.0095 inch was specified. Bearings were oriented such that each bearing would be loaded into the pivot at rated power, even though load angles were different for each bearing.

The compressor was modified and retested. The retesting at previous test points and other operating and nonoperating points revealed only synchronous frequencies. All signs of subsynchronous frequencies were removed.

DISCUSSION

There are two areas for further investigation as a result of this problem and subsequent analysis. First is the observation of two distinct subsynchronous frequencies. Allis-Chalmers' analysis predicted the higher frequency of approximately 3100 cpm quite well; however, the frequency of major amplitude occurred at approximately 2700 cpm. Allis-Chalmers had not seen this type of double subsynchronous frequency previously on a conventional midspan compressor rotor. It is assumed to have been generated as a result of unequal bearing loadings compounded by the magnitude of levels of subsynchronous vibration. A point of interest is that the lower frequency agrees reasonably well with a peak on the synchronous response curve (fig. 17).

Second, and most disconcerting, is the fact that subsynchronous instabilities did develop despite the substantial values of the log decrement. Even if one were to increase the destabilizing force four times, a log decrement of approximately 0.3 would still exist. There are many conventional midspan rotors with log decrements much lower than this value with equal or higher destabilizing force values that have a history of successful operation. It is postulated that some not-yet-defined level of excitation exists on this type of rotor. There are several possibilities:

(1) Gear error effects - No attempt has been made to add any destabilizing force as a result of gear inaccuracies or torsional-lateral coupling.

(2) Effects of open impellers - The impeller on this pinion was of an uncovered design. It is physically impossible to assure operation of this type of impeller with uniform circumferential and axial clearances. Perhaps the nonuniform clearances along with the turbulent bypass effects from blade to blade are generating much higher destabilizing forces than normally associated with a

closed impeller. In addition, other aerodynamic factors such as flow separation and stall have not been quantified as to their destabilizing influence.

It is worth noting that our experiences are in reasonable agreement with data presented in reference 7.

CONCLUSIONS

1. A subsynchronous instability existed on a geared, overhung rotor. State-of-the-art rotor dynamics analysis techniques provided a reasonable analytical model of the rotor. A bearing modification, arrived at analytically, was made to the compressor and eliminated the instability.

2. Further research is required to more accurately define the mechanism and to quantify the forces which cause the instability.

REFERENCES

1. Rouch, K. E.; and Kao, J. S.: Reduction in Rotor Dynamics by the Finite Element Method. ASME Paper 79-DET-70, 1979.

2. Rouch, K. E.; and Kao, J. S.: A Tapered Beam Finite Element for Rotor Dynamic Analysis. J. Sound Vibr., 1979, vol. 66, no. 1, pp. 119-140.

3. Wittman, L. J.: Compressor Division Engineering Report 16-ER-416. November 13, 1978.

4. Alford, J. S.: Protecting Turbomachinery from Self-Excited Rotor Whirl. J. Eng. Power, Trans. ASME Series A, vol. 87, October 1965, pp. 333-334.

5. Brown, J. M: Lateral and Torsional Stiffness of Shafts of Varying Diameter. Doctoral thesis, Purdue University, 1952.

6. Jones, G. J.; and Martin, F. A.: Geometry Effects in Tilt Pad Journal Bearings, Paper AT449/80, Glacier Publication.

7. Pennink, Hans: The State of the Art of High Speed Overhung Centrifugal Compressors for the Process Industry. Proceedings of 7th Turbomachinery Symposium.

8. Lund, J. W.: Stability and Damped Critical Speeds of a Flexible Rotor in Fluid Film Bearings. ASME Paper 73-DET-103, 1973.

TABLE 1

	LOW SPEED	HIGH SPEED
SPEED (RPM)	8057	9400
HORSEPOWER (BHP)	3774	4226
BEARING LOADS (POUNDS$_{FORCE}$)	1114 DOWNWARD 1ST STAGE	432 DOWNWARD 2ND STAGE
STATIC (WEIGHT)	242 UPWARD THRUST BRG.	352 DOWNWARD 3RD STAGE
TOTAL (WEIGHT AND GEAR REACTIONS)	1782 $\angle 17°$ 1ST STAGE	3560 $10.5°$ 2ND STAGE
	3487 $28°$ THRUST BRG.	3936 $27°$ 3RD STAGE
JOURNAL DIAMETER (IN.)	4.0	4.0
LENGTH (IN.)	3.0	3.0
DIAMETRAL CLEARANCE INCLUDING JOURNAL TOLERANCE (IN.)	.007/.010	.007/.010
m (BEARING PRELOAD)	.33	.33
BEARING TYPE	5 PAD TILT PAD CENTRAL PIVOT	5 PAD TILT PAD CENTRAL PIVOT
LUBRICANT	215 SSU @ 100°F VI = 95	

TABLE 2

Case #	Description	BEARING - 1ST STAGE Dia. (In.)	L/D	Dia. Clr.(In.)	Load Dir.	BEARING - BLIND SIDE Dia. (In.)	L/D	Dia. Clr.(In.)	Load Dir.	Aero Q(lb/in)	Freq. (CPM)	Prec.	Log Dec	Comments
1	Original Configuration	4.0	.75	.0084	18° Off Pivot	4.0	.75	.0084	8° Off Pivot	0	3151	Fwd.	.3666	$m = .285$
2	Org.Configuration	4.0	.75	.0084	18° Off Pivot	4.0	.75	.0084	9° Off Pivot	10,000.	3185	Fwd.	.136	$m = .285$
3	Org.Configuration	4.0	.75	.0084	18° Off Pivot	4.0	.75	.0084	8° Off Pivot	16,000.	3195	Fwd.	.0004	$m = .285$
4	Rotated Brg. load Into Pivot	4.0	.75	.0084	Into Pivot	4.0	.75	.0084	Into Pivot	16,000.	3014	Fwd.	.0071	$m = .285$
5	Rotated Brg. Load Between Pivot	4.0	.75	.0084	Between Pivot	4.0	.75	.0084	Between Pivot	16,000.	3288	Fwd.	.0026	$m = .285$
6	2" Shorter Overhang	4.0	.75	.0084	18° Off Pivot	4.0	.75	.0084	8° Off Pivot	16,000.	3596	Fwd.	.184	$m = .285$
7	Final Fix w/ L/D = 1 Brg.	4.0	1.0	.0085	Into Pivot	4.0	1.0	.0085	Into Pivot	16,000.	3086	Fwd.	.082	$m = .2$
8	Alternate Arrangemt. w/ L/D = 1 Brg.	4.0	1.0	.0085	Between Pivot	4.0	1.0	.0085	Between Pivot	16,000	3261	Fwd.	.054	$m = .2$
9	Stiffer Shaft 4.5 Brg o Shaft	4.5	.75	.0095	18° Off Pivot	4.5	.75	.0095	8° Off Pivot	16,000	3275	Fwd.	.181	$m = .2$
10	Stiffer Shaft 4.5 Brg & Shaft	4.5	.75	.0095	Into Pivot	4.5	.75	.0995	Into Pivot	16,000	3189	Fwd.	.168	$m = .2$
11	Case 7 w/reduced oil temp. 140°	4.0	1.0	.0085	Into Pivot	4.0	1.0	.0085	Into Pivot	16,000	3151.4	Fwd.	.1161	$m = .2$
12	Case 7 w/reduced oil temp. 120°	4.0	1.0	.0085	Into Pivot	4.0	1.0	.0005	Into Pivot	16,000	3328	Fwd.	.0764	$m = .2$

For L/D = .75 orientation makes essentially no difference. (Cases 3–5)

CRITICAL SPEED MAP
12 JUN 75
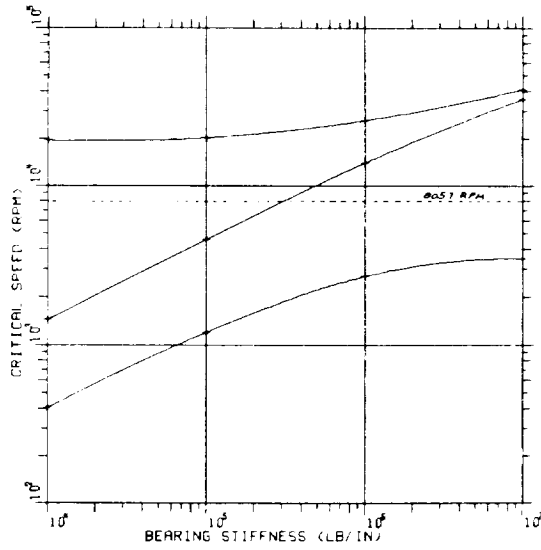
LOW SPEED PINION

ASSUMES EQUAL STIFFNESS

Figure 1

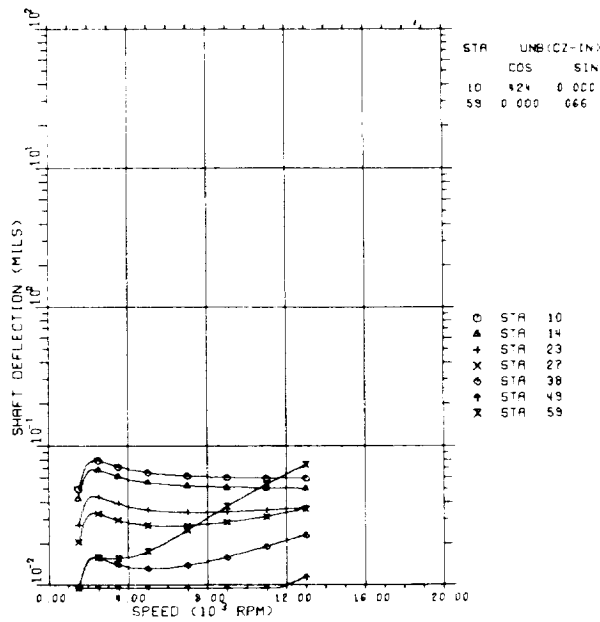ROTOR MODE SHAPE AT CRITICAL SPEED
PROGRAM 8166-001
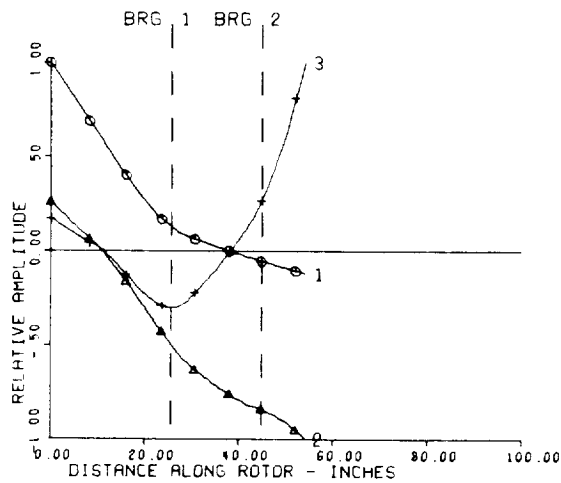
DATE
12 JUN 75

BRG BRG
NO   STIFF
1   1×10^6
2   1×10^6

CRITICAL SPEED
1   2687 RPM
2   14029 RPM
3   26044 RPM

LOW SPEED PINION

Figure 2

75

CIRCULAR ORBIT ROTOR UNBALANCE RESPONSE
PROGRAM 8166-002
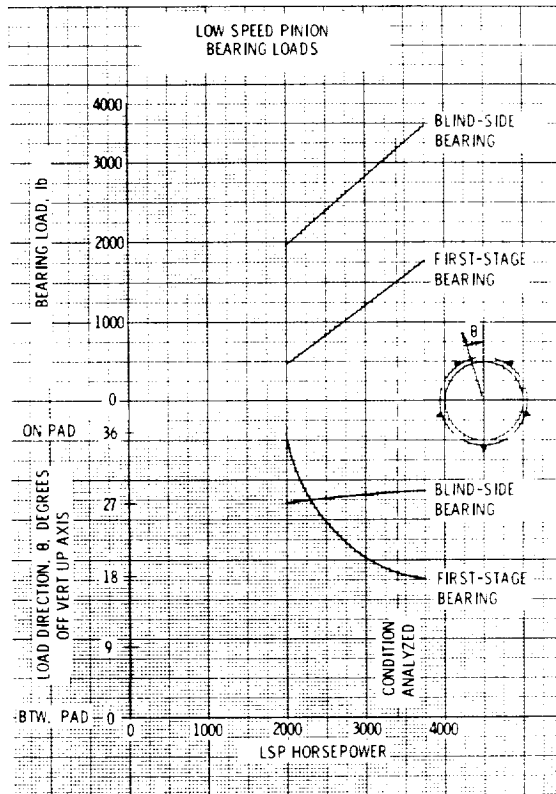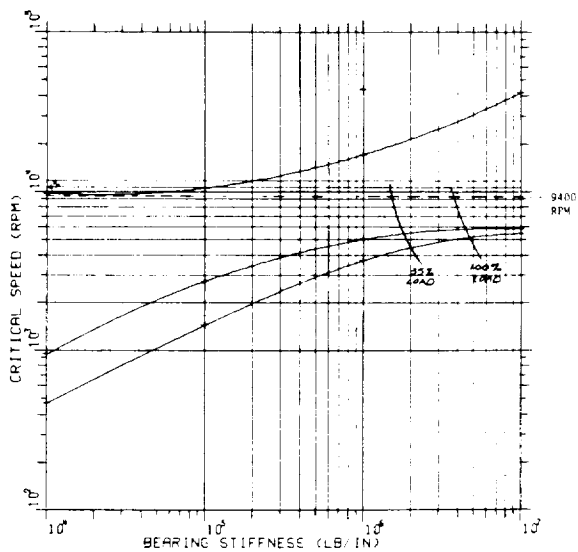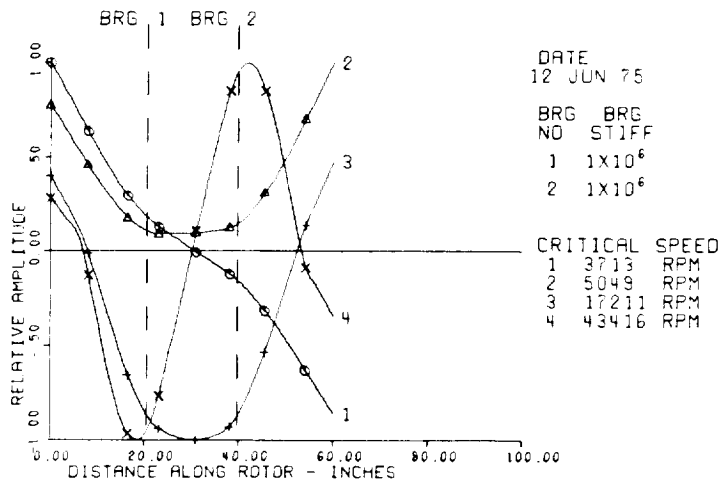12 DEC 75

L.S. PINION

Figure 3

LOW SPEED PINION
BEARING LOADS

Figure 4

76

CRITICAL SPEED MAP
12 JUN 75

HIGH SPEED PINION

Figure 5

ROTOR MODE SHAPE AT CRITICAL SPEED
PROGRAM 8166-001

HIGH SPEED PINION

Figure 6

77

ROTOR MODE SHAPE AT CRITICAL SPEED
PROGRAM 8166-001
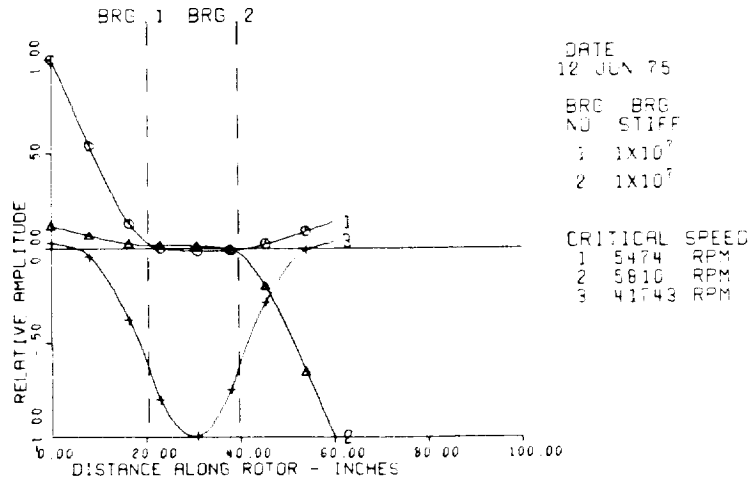
HIGH SPEED PINION

Figure 7

CIRCULAR ORBIT ROTOR UNBALANCE RESPONSE
PROGRAM 8166-002
27 JUN 75

HIGH SPEED PINION

Figure 8

78

Figure 9

Figure 10

3075 RPM
0.48 MILS

6065 RPM
0.54 MILS

Figure 11

3120 RPM
0.41 MILS

2880 RPM
0.16 MILS

6040 RPM
0.50 MILS

Figure 12

2670 RPM
1.66 MILS

3090 RPM
0.62 MILS

6040 RPM
0.56 MILS

Figure 13

80

LOW SPEED PINION
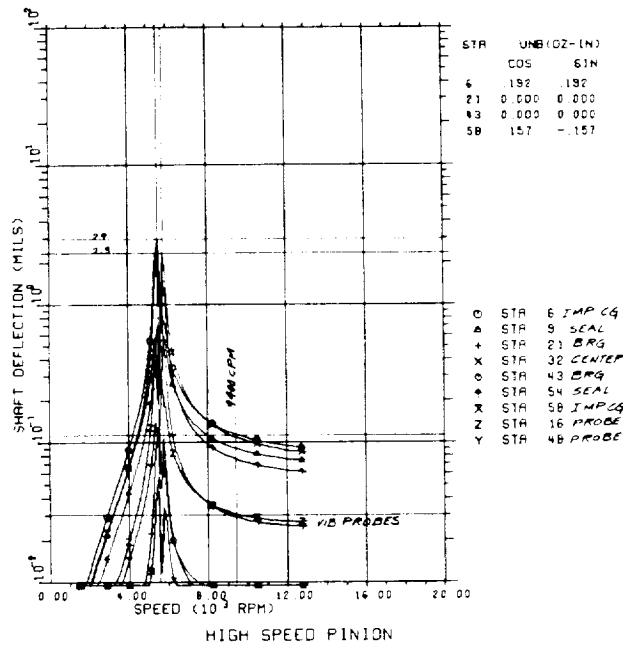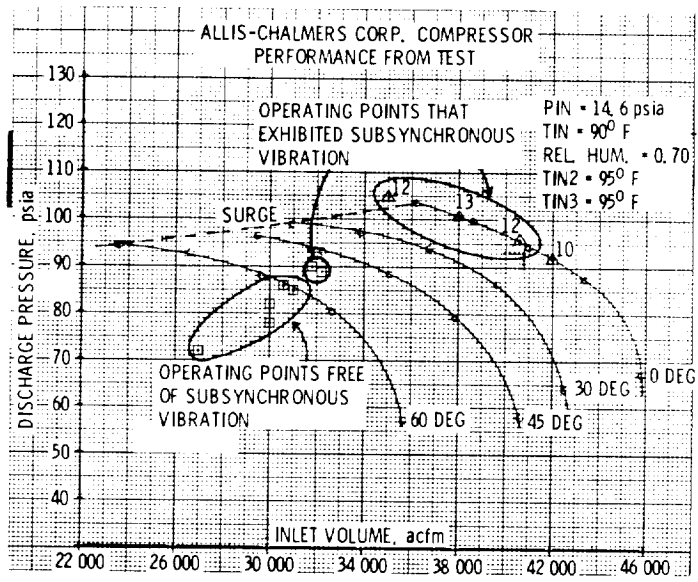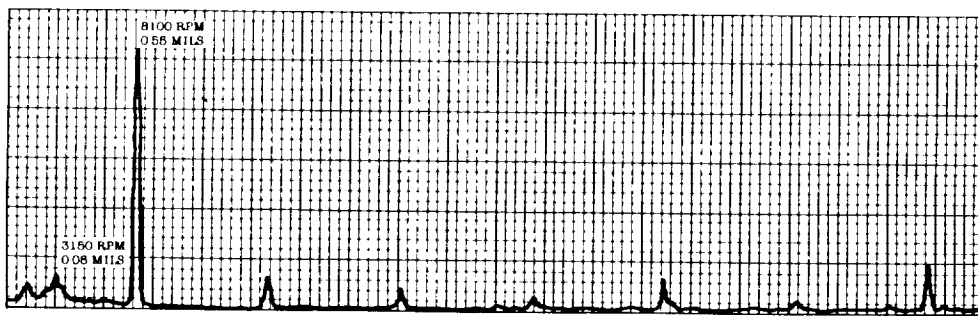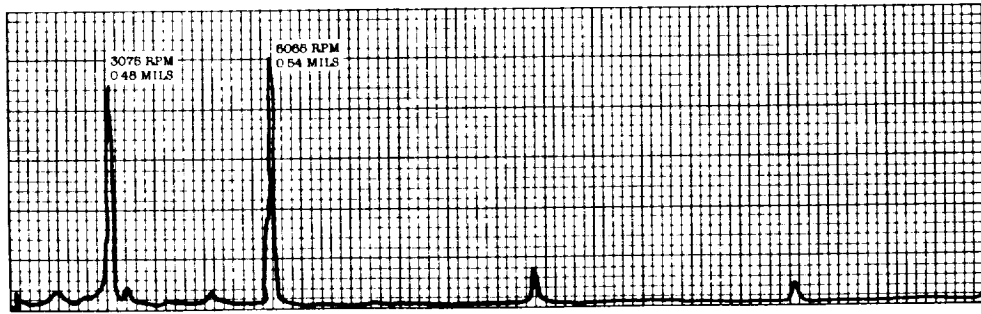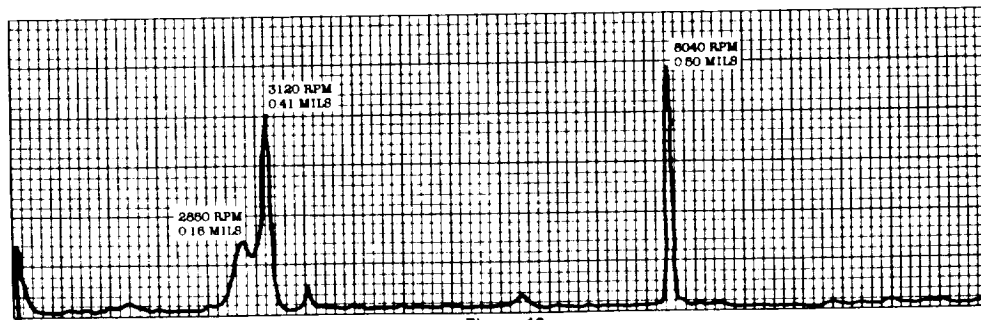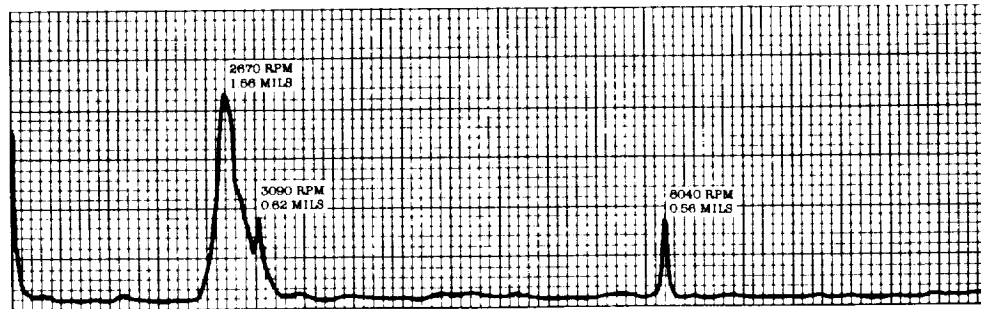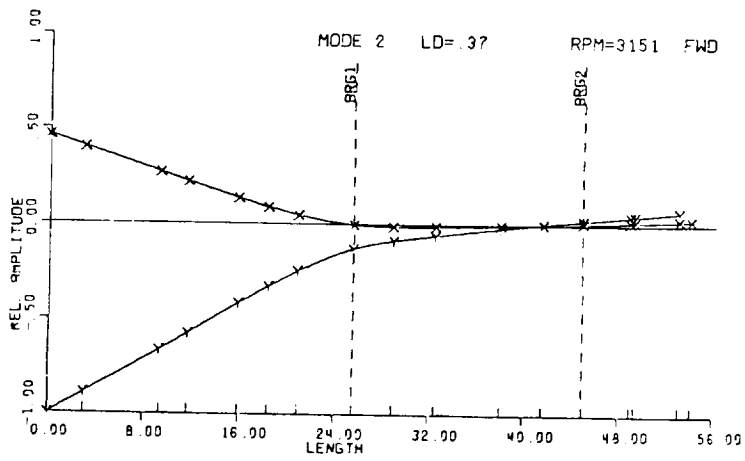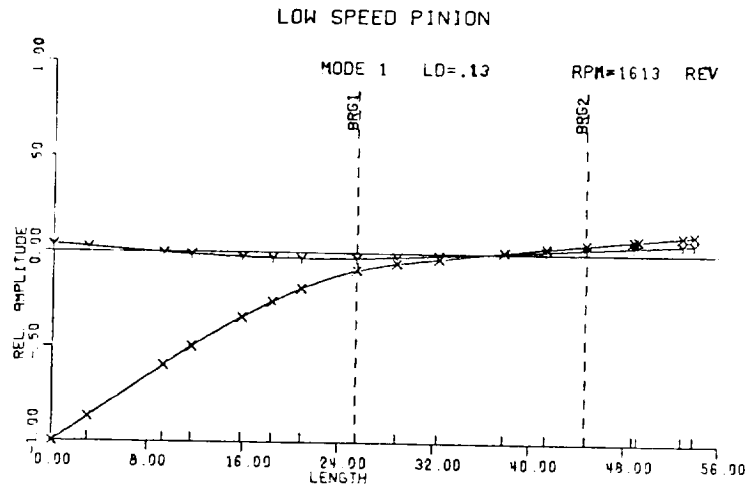
Figure 14

FIRST-STAGE BEARING
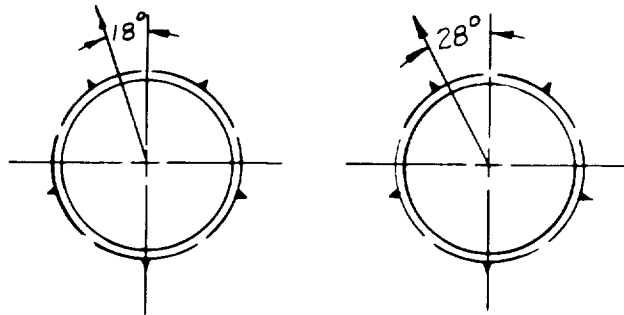LOAD DIRECTION

BLIND-SIDE BEARING
LOAD DIRECTION

Figure 15

OVERHUNG GEAR COMPRESSOR — UNDAMPED
VERTICAL CRITICAL SPEEDS

CRITICAL SPEED SEARCH

CRITICAL #	BRG #1 STIFFNESS LB/IN	BRG #2 STIFFNESS LB/IN
1	968,170	463,540
2	714,580	2,525,200

ROTOR MODE SHAPE AT CRITICAL SPEED

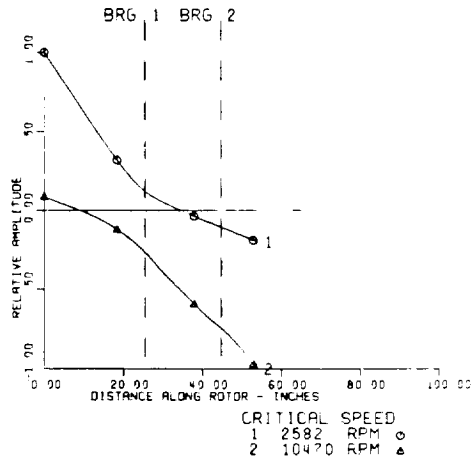CRITICAL SPEED
1 2582 RPM ○
2 10470 RPM △

Figure 16

OVERHUNG GEAR COMPRESSOR
SYNCH. RESPONSE AT IMPELLER
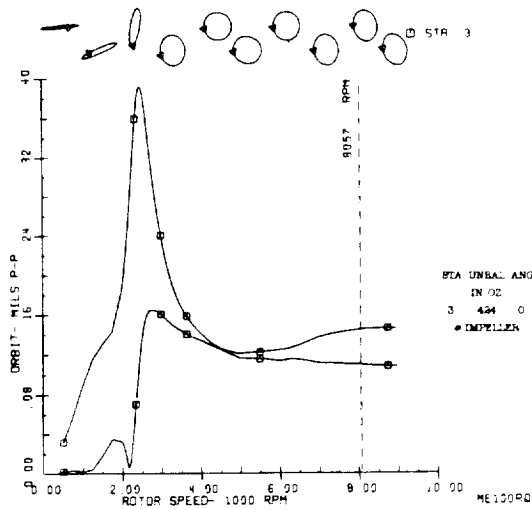(UNBALANCE BASED ON 10% OF ROTOR WEIGHT)
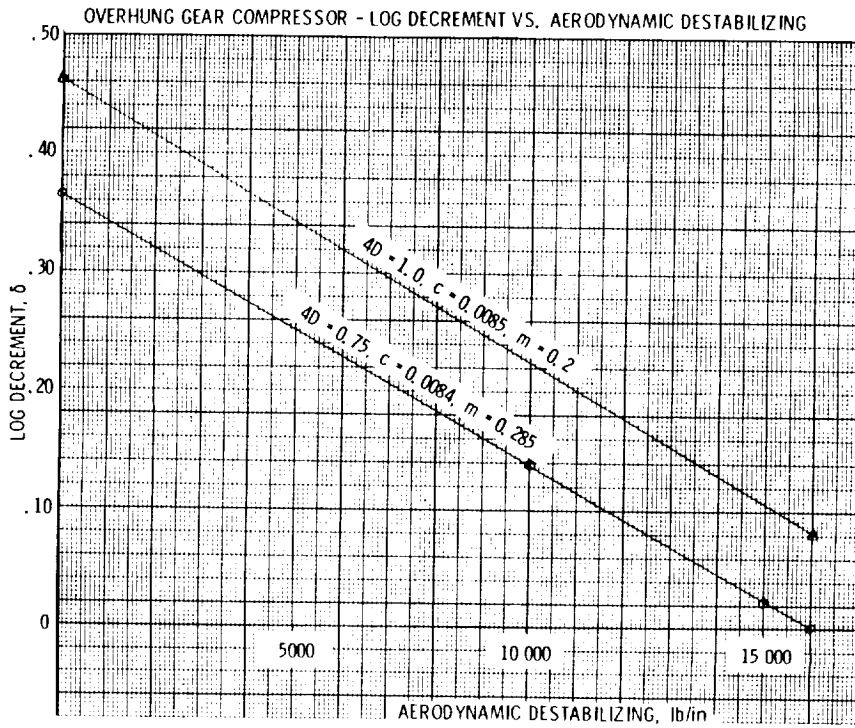EXTERNAL FORCES DUE TO GEAR INCLUDED.

Figure 17

82

OVERHUNG GEAR COMPRESSOR - LOG DECREMENT VS. AERODYNAMIC DESTABILIZING

Figure 18